Technical Note: Procedure for the calibration and validation of kilo-voltage cone-beam CT models

Gloria Vilches-Freixas and Jean Michel Létang
*Université de Lyon, CREATIS, CNRS UMR5220, Inserm U1206, INSA-Lyon, Université Lyon 1,
Centre Léon Bérard, Lyon 69373 Cedex 08, France*

Sébastien Brousmiche
Ion Beam Application, Louvain-la-Neuve 1348, Belgium

Edward Romero and Marc Vila Oliva
*Université de Lyon, CREATIS, CNRS UMR5220, Inserm U1206, INSA-Lyon, Université Lyon 1,
Centre Léon Bérard, Lyon 69373 Cedex 08, France and Ion Beam Application,
Louvain-la-Neuve 1348, Belgium*

Daniel Kellner, Heinz Deutschmann, Peter Keuschnigg, and Philipp Steininger
*Institute for Research and Development on Advanced Radiation Technologies, Paracelsus Medical University,
Salzburg 5020, Austria*

Simon Rit[a)]
*Université de Lyon, CREATIS, CNRS UMR5220, Inserm U1206, INSA-Lyon, Université Lyon 1,
Centre Léon Bérard, Lyon 69373 Cedex 08, France*

Purpose: The aim of this work is to propose a general and simple procedure for the calibration and validation of kilo-voltage cone-beam CT (kV CBCT) models against experimental data.
Methods: The calibration and validation of the CT model is a two-step procedure: the source model then the detector model. The source is described by the direction dependent photon energy spectrum at each voltage while the detector is described by the pixel intensity value as a function of the direction and the energy of incident photons. The measurements for the source consist of a series of dose measurements in air performed at each voltage with varying filter thicknesses and materials in front of the x-ray tube. The measurements for the detector are acquisitions of projection images using the same filters and several tube voltages. The proposed procedure has been applied to calibrate and assess the accuracy of simple models of the source and the detector of three commercial kV CBCT units. If the CBCT system models had been calibrated differently, the current procedure would have been exclusively used to validate the models. Several high-purity attenuation filters of aluminum, copper, and silver combined with a dosimeter which is sensitive to the range of voltages of interest were used. A sensitivity analysis of the model has also been conducted for each parameter of the source and the detector models.
Results: Average deviations between experimental and theoretical dose values are below 1.5% after calibration for the three x-ray sources. The predicted energy deposited in the detector agrees with experimental data within 4% for all imaging systems.
Conclusions: The authors developed and applied an experimental procedure to calibrate and validate any model of the source and the detector of a CBCT unit. The present protocol has been successfully applied to three x-ray imaging systems. The minimum requirements in terms of material and equipment would make its implementation suitable in most clinical environments. © 2016 American Association of Physicists in Medicine. [http://dx.doi.org/10.1118/1.4961400]

1. INTRODUCTION

Several devices have been developed to acquire images of the patient in the treatment room for image-guided radiation therapy (IGRT). Kilo-voltage (kV) cone-beam computed tomography (CBCT) provides volumetric images of the patient to correct for the treatment position and to assess changes in the internal anatomy. Implementation of dual-energy capabilities in CBCT units is finding application in diagnostics to improve material segmentation and enhance contrast. A model of the

kV CBCT unit is required to optimize the imaging device, to simulate and correct for scatter radiations,[1] to optimize single[2] and dual-energy acquisition protocols, to compute the patient imaging dose,[3] and for material decomposition in dual-energy CT.

Verification of CBCT models has been carried out in different manners in the literature.[3] To validate the x-ray source model, some authors performed half-value layer (HVL) measurements,[1,4] but only the first HVL is commonly checked. In a recent work,[5] the authors proposed an original

experimental setup to rapidly characterize x-ray sources by acquiring angular-dependent HVLs and fluence data. Others compared the Monte Carlo calculations with measured depth dose distributions and dose profiles.[6,7] A solution to validate the detector model is the method proposed by Granton *et al.*[8] which consists of recording image intensities over a wide range of x-ray tube voltages and comparing them to predicted image intensities using the source and the detector models.

Even though some works in the literature have assessed either the accuracy of the source model or the detector model separately, the authors believe that it is necessary to provide a general procedure to validate both models in a simple manner. The purpose of this study is to propose a concise experimental approach to calibrate and validate a given model for the source and the detector of a CBCT scanner. If the model is precalibrated or if precise manufacturer information is available, the degrees of freedom of the model tend to zero and, then, this procedure can be used exclusively for model validation. As an example of application, the proposed method has been applied to the models of three different CBCT scanners and the results are discussed.

2. MATERIALS AND METHODS

2.A. Procedure

The calibration and validation of the CT model is a two-step protocol: the source model then the detector model. The source model at each voltage is represented by the photon energy spectrum $\Phi_{0,k}(E,\theta,\phi)$, i.e., the number of photons per energy E for the kth voltage and without additional filtration (index 0) in a direction (θ,ϕ) expressed in spherical coordinates. The detector model is represented by the detector response $S_p(E,\beta)$ which is defined for each pixel p and is a function of the incident photon energy E and the angle β between the normal to the detector and the incident ray.

2.A.1. Source

The procedure to validate the source model is as follows: first, a series of dose measurements in air is performed with varying filter thicknesses and materials in front of the source. High-purity sheets of aluminum (Al), copper (Cu), and silver (Ag) are used. This procedure is repeated for several tube voltages (kV), tube current (mA), and exposure times (ms). The absorbed dose in air $D_{j,k}^{\text{exp}}$ of the jth setup of filters ($j = 1,\dots,J$) and kth voltage is measured using a dosimeter working in the range of energies of interest. The energy dependence of the dosimeter used for the experimental measurements is assumed to be negligible at this range of voltages. The theoretical dose in air is calculated using

$$D_{j,k}^{\text{theo}}(\theta,\phi) = \sum_i (\mu_{\text{en}}/\rho)_{\text{air}}(E_i) \cdot \Phi_{j,k}(E_i,\theta,\phi) \cdot E_i, \quad (1)$$

where $D_{j,k}^{\text{theo}}$ is the theoretical dose in air, i is the index of energy bins of the spectrum with E_i the corresponding energy, $(\mu_{\text{en}}/\rho)_{\text{air}}$ is the energy-dependent mass energy absorption coefficient of air taken from the NIST database,[9] and $\Phi_{j,k}$

is the polychromatic spectrum of the jth setup computed from $\Phi_{0,k}$ and the known thicknesses of filters. A subset of acquired data, e.g., dose measurements without filter in front of the source ($j = 0$), might be used for calibrating the source model. The last step of the validation process consists of giving a figure of merit (e.g., the percentage relative difference) of the comparison between experimental and calculated dose values for each voltage, filter material, and filter thickness.

The proposed method can be used to perform both a single point dose comparison (e.g., $\theta = 0°, \phi = 0°$) and a two-dimensional (2-D) dose comparison (θ,ϕ). For the latter, the irradiation area is discretized and the validation procedure repeated by shifting the dosimeter accordingly (step-and-shoot technique). Another option is to substitute the punctual dosimeter by a 2-D dosimetric film or an array detector.

2.A.2. Detector

The validation of the detector model assumes that the source model is calibrated and validated. A set of image acquisitions is performed with varying filter materials and tube voltages. Like the source validation procedure, high-purity sheets of aluminum, copper, and silver are placed in the beam to modify the source spectra $\Phi_{0,k}$. For each setup j ($j = 1,\dots,J$), more than 500 frames are acquired to reach the plateau-regime of the lag.[10] A temporal median is then performed over the last frames where the image intensity remains constant (i.e., the last 100 frames) to compute the measured pixel value $P_{j,k}^{\text{exp}}(p)$. The predicted pixel values are determined as follows:

$$P_{j,k}^{\text{theo}}(p) = \sum_i \Phi_{j,k}(E_i,\theta_p,\phi_p) \cdot S_p(E_i,\beta_p), \quad (2)$$

where $P_{j,k}^{\text{theo}}(p)$ is the predicted pixel value for the jth filter setup and the kth voltage, θ_p and ϕ_p are the spherical coordinates of pixel p in the coordinate system of the source, $S_p(E_i,\beta_p)$ the detector response at energy E_i and β_p, which is uniquely defined by the scanner geometry and (θ_p,ϕ_p). Parameters of the detector model might be calibrated against a subset of experimental data if necessary. Then, predicted and measured pixel values for each voltage and spectrum filtration are compared using a goodness of fit indicator, such as the percentage relative difference.

The detector response (total absorbed energy) is considered locally deposited, and not spread like it should be if scatter in the detector was accounted for.[11] Consequently, Eq. (2) can only be used to validate the energy response of the detector, not its spatial response.

2.B. Application

2.B.1. Experimental setups

The current procedure was applied to the three kV-CBCT scanners of Table I. All flat panel detectors had CsI:Tl scintillators. The filters in front of the x-ray source were slabs of aluminum (nominal thicknesses: 0.5, 1, and 2 mm), copper (nominal thickness: 0.1 mm), and silver (nominal thickness:

TABLE I. kV-CBCT units.

#	System	X-ray tube	Flat panel
1	Elekta XVI	Dunlee D604	Perkin Elmer XDR1622(Al)
2	medPhoton ImagingRing	IAE RTM70HS	Perkin Elmer XDR1642(Al)
3	IBA PT Gantry CBCT test bench	Varian GS2075	Thales Pixium4343RF

0.125 mm). All filters were of high-purity (≥99.9%). The exact thickness t of each high-purity filter material of known density ρ was obtained from precise measurements of the mass m and the area A. Moreover, two dosimeters working in the range of voltages of interest, i.e., from 50 to 130 kV, specifically the Nomex (PTW GmbH, Freiburg, Germany) and the MagicMax (Ion Beam Applications S.A., Louvain-la-Neuve, Belgium) multimeters, were used for the source model verification. Acquisitions were performed with three filter combinations: (f_1) no filter, (f_2) 8 mm Al, and (f_3) 0.3 mm Cu + 0.5 mm Ag.

A prerequisite of implementing this procedure is to have a model that needs to be validated. The proposed method can be used with any given model of source and detector response. To illustrate its application, a model for the source and for the detector response is proposed below. The unknown parameters of the models are determined through calibration against experimental data. Finally, the agreement between the experimental data and the model output is measured by quantifying the relative differences between the measures and the predictions.

2.B.2. Source model

Proprietary information, such as the inherent filtration (stoichiometric composition and thickness) and the anode angle of the x-ray source, is either not provided or it is given with large uncertainties. To overcome this restriction, the unknown tube filtration of the systems under study was described as a linear combination of two known materials. Aluminum (Al) and copper (Cu) were chosen as basis because they are commonly employed in commercial x-ray tubes as filter materials. In this study, the x-ray source was modeled by a photon energy spectrum parameterized by the anode angle, the tube voltage, and the thicknesses of the basis materials (Al, Cu) which represent the inherent filtration. Using the program SpekCalc,[12] photon fluence spectra were generated without any filtration for different voltages at 10 kV step and for anode angles from 5° to 22° at 1° interval. Then, each spectrum was filtered with all possible thickness combinations of Al (from 0.1 to 8.0 mm at 0.1 mm step) and Cu (from 0.005 to 0.5 mm at 0.005 mm

TABLE II. Model parameters of each imaging system (see Table I) determined through minimization.

System	Anode angle (deg)	mm Al	mm Cu	CsI length (μm)
#1	18	7.2	0.01	750
#2	11	0.3	0.06	350
#3	11	3.0	0.01	450

step). Finally, the experimental data were used to calibrate the model. The optimal tuple of parameters for each imaging system (anode angle, Al and Cu thicknesses) was determined by minimizing the following cost function:

$$F_{\text{source}} = \sum_{j,k} \left(\frac{D_{j,k}^{\text{exp}} - D_{j,k}^{\text{theo}}}{D_{j,k}^{\text{exp}}} \right)^2, \tag{3}$$

where the index j and k refers to the jth filter setup and kth voltage, respectively. $D_{j,k}^{\text{exp}}$ are the experimental dose values and $D_{j,k}^{\text{theo}}$ are the theoretically determined dose values.

Dose measurements were carried out with a narrow beam geometry using: the filter cassette M2 (system #1), the dynamic collimation jaws (system #2), and lead slabs (system #3). A dosimeter was attached to the flat panel detector and placed at the central beam axis. Thus, only the spectrum along the beam central axis ($\theta = 0°$) was considered. The absolute photon yield was adjusted by weighting the SpekCalc spectra, filtered only with the inherent filtration, with the ratio of measured and theoretical dose in air without additional filtration ($j = 0$) for the corresponding (kV, mA, ms) tuple of source parameters.

2.B.3. Detector response model

The detector response was modeled as the average contribution to the pixel value of one incident photon as a function of its energy. It was assumed that pixel values were proportional to the energy deposit in the scintillator. The detector response was generated using Monte Carlo simulations. The flat panel detector was modeled in GATE (Ref. 13) v7.2 (based on GEANT4
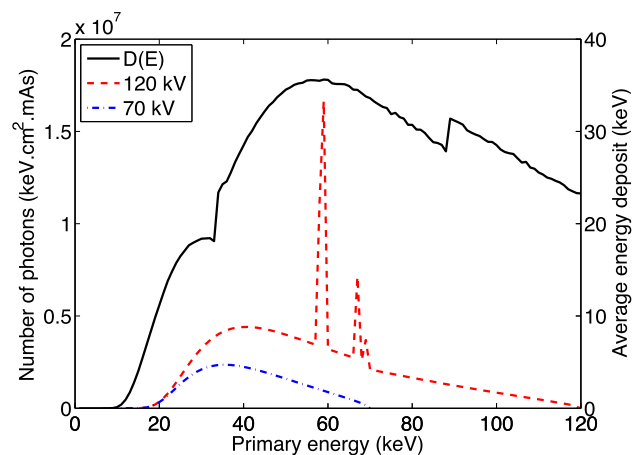

FIG. 1. Source and detector response models built for the kV-CBCT unit of system #3 (see Table I). Left axis: plot of the 70 and 120 kV x-ray source spectra. Right axis: Monte Carlo simulated detector response in energy.

TABLE III. For all systems (see Table I), results of the source and the detector model verification expressed in terms of the relative difference (in %) averaged over all voltages. The total relative difference, averaged over all filtration, and the relative to each filtration are shown in separate columns.

System	Source			Detector			
	Total	f_1	f_3	Total	f_1	f_2	f_3
#1	1.4 ± 5.1	2.9 ± 1.7	−12 ± 5.4	1.8 ± 6.5	−2.1 ± 2.4	4.0 ± 1.3	3.6 ± 10
#2	−0.48 ± 3.5	−1.2 ± 1.6	0.78 ± 5.1	−3.7 ± 9.9	−2.3 ± 4.0	−2.8 ± 5.8	−6.9 ± 19
#3	0.45 ± 2.8	0.97 ± 2.1	−6.3 ± 1.1	−2.4 ± 5.7	−0.86 ± 1.3	0.63 ± 4.2	−7.5 ± 7.3

v10.1, physics list: emlivermore) as a stack of layers of user-defined materials according to the manufacturer's description (stoichiometry and thickness). The response of the detector was obtained by measuring the energy deposited in the scintillator layer with monoenergetic pencil beams of energies ranging from 1 to 140 keV,[14] perpendicular to the detector. In the 20–140 keV energy range, the statistical uncertainty of the simulated detector response was below 0.5% for all detectors (10^{10} photons). To provide an absolute value of the deposited energy on the detector, no calibration nor corrections, i.e., bad pixels and gain, was applied to the acquired projections, only offset correction. Then, a parameter was used in the model to relate the detector signal to the predicted value, i.e., a multiplicative factor δ_p for each pixel p of the detector determined in the least square sense

$$\delta_P = \frac{\sum_{j,k} P_{j,k}^{\text{theo}}(p)}{\sum_{j,k} P_{j,k}^{\text{exp}}(p)}. \tag{4}$$

$P_{j,k}^{\text{theo}}(p)$ is the predicted pixel value for setup jth and kth voltage with p the pixel index and $P_{j,k}^{\text{exp}}(p)$ the measured pixel value for setup jth and kth voltage. To manage bad pixels, $P_{j,k}^{\text{exp}}(p)$ was determined by taking the spatial median of the signal in a 3×3 pixels area perpendicular to the beam central axis. Moreover, as the exact thickness of the CsI scintillator layer was not perfectly known, the detector response was computed for scintillator lengths ranging from 200 to 900 μm at steps of 50 μm. The experimental data were used to determine the optimal CsI length that minimized the following cost function:

$$F_{\text{detector}} = \sum_{j,k} \left(\frac{\delta_p P_{j,k}^{\text{exp}} - P_{j,k}^{\text{theo}}}{\delta_p P_{j,k}^{\text{exp}}} \right)^2, \tag{5}$$

where the index j and k refers to the setup jth and kth voltage, respectively.

2.B.4. Sensitivity analysis

The term "sensitivity analysis" refers here to the study of the variations of the model accuracy (cost function) around its optimum. In particular, once the optimal tuple of source model values (mm Al, mm Cu, anode angle) was determined for each system, small variations (i.e., up to ±0.3 mm Al, ±0.01 mm Cu, ±3°) around the optimal values at a time were introduced for

each parameter. For the detector response model, the scintillator length was varied from 200 to 900 μm.

3. RESULTS

The source model was calibrated using dose measurements in air with increasing thicknesses of aluminum, with the beam filtrations f_1 (no filter) and f_3 (0.3 mm Cu + 0.5 mm Ag). For each imaging system, the parameters of the source model were determined by minimizing the cost function described in Eq. (3) and are summarized in Table II. In Fig. 1, a plot of two representative x-ray spectra and the detector response in energy, obtained after calibration, for system #3 is shown.

The results of the point-by-point dose comparison between experimental and theoretical values are summarized in Table III. This is illustrated visually in Fig. 2 for the system #3. The figures for the other systems are provided as supplementary material.[15] Averaging over all setups, all imaging systems showed an agreement between theoretical absorbed dose in the dosimeter and measurements within 1.5%.

For the detector response verification, three irradiation setups were evaluated: f_1 (no filter), f_2 (8 mm Al), and f_3 (0.3 mm Cu + 0.5 mm Ag). For each imaging system, the scintillator length, which was an unknown parameter of the detector model, was determined by minimizing the cost function described in Eq. (5). The resulting CsI lengths are shown in Table II. The results of the detector response model verification are summarized in Table III and it is illustrated in Fig. 3 for the system #3. In general, good agreement between
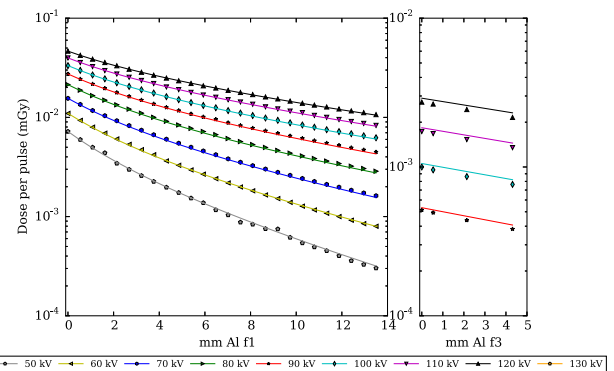

FIG. 2. Results of the source model verification for the imaging system #3 (see Table I). Semi-logarithmic plot of the absolute dose per pulse as a function of the aluminum thickness interposed in the beam for several tube voltages. Left: Original beam spectra (i.e., filtration f_1); right: spectra with filtration f_3. Markers represent the experimental dose readouts and the continuous lines the theoretical dose values.
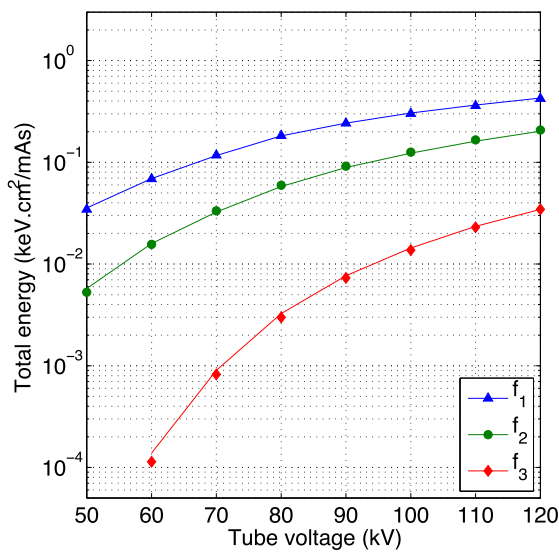
FIG. 3. Results of the detector response verification for the imaging system #3 (see Table I). Semi-logarithmic plot of the theoretical (continuous line) and measured (markers) energy deposited in the detector for increasing x-ray tube potentials divided by the mAs. The method was repeated using different spectra filtration: f_1, f_2, f_3.

the theoretical and the measured energy deposited in the detector is obtained for setup f_1 and f_2. For the setup f_3, larger discrepancies are observed, particularly for the imaging system #2. Nevertheless, when taking into account all the setups, the theoretical total energy deposit in the detector agreed with measurements to within 4% for all imaging systems.

The results of the sensitivity analysis for the three imaging systems are shown in Fig. 4. Systems #2 and #3 are more sensitive to variations in the anode angle, inherent filtration, and scintillator length than system #1.

4. DISCUSSION

In this work, an experimental procedure has been developed to calibrate and validate any model of source and detector responses of a CBCT unit.

In the application example, the unknown parameters of the models were determined by minimizing a defined cost-function using the procedure measurements. The results of the source model verification showed worse agreement of the f_3 filter setup for the imaging system #1 compared to the others. Either the process of minimizing the cost function did not provide the optimal inherent filtration thicknesses, because there were fewer data points in f_3 compared to f_1, or the f_3 data set points out an error in the model for highly hardened beams. In the detector model verification, larger discrepancies were observed for the setup f_3, particularly for the imaging system #2. This could be due to a limitation or error in the model, e.g., a wrong density or thickness estimation in the simulated stack of layers. Nevertheless, even if the source model accuracy for the different setups was not optimal, it seems to have little influence on the detector model accuracy.

The main difference between our method and those found in the literature is that we generate many data points using different filtering materials. Moreover, the measurement and the prediction of doses in air are compared for each filter setup instead of comparing the HVLs only. Due to the discontinuities in the spectrum range, materials such as silver, gold, and tungsten modulate the initial spectra in a different way compared to aluminum. The introduction of copper and silver filtration in the verification process seems to highlight errors or limitations in the source and in the detector model that were not noticeable with the aluminum filtration only.

The materials required to set the experimental framework are easily accessible and often available in hospitals, i.e., attenuation filters of different materials for both models, and a dosimeter working in the range of CT imaging voltages. This procedure is interesting for the physicists who need a forward model benchmarked against experimental data, a prerequisite in many applications, some of which have been listed in the Introduction.

The protocol has only been illustrated to a single direction for the source and the detector of three CBCT scanners but other directions may be validated by repeating the procedure,
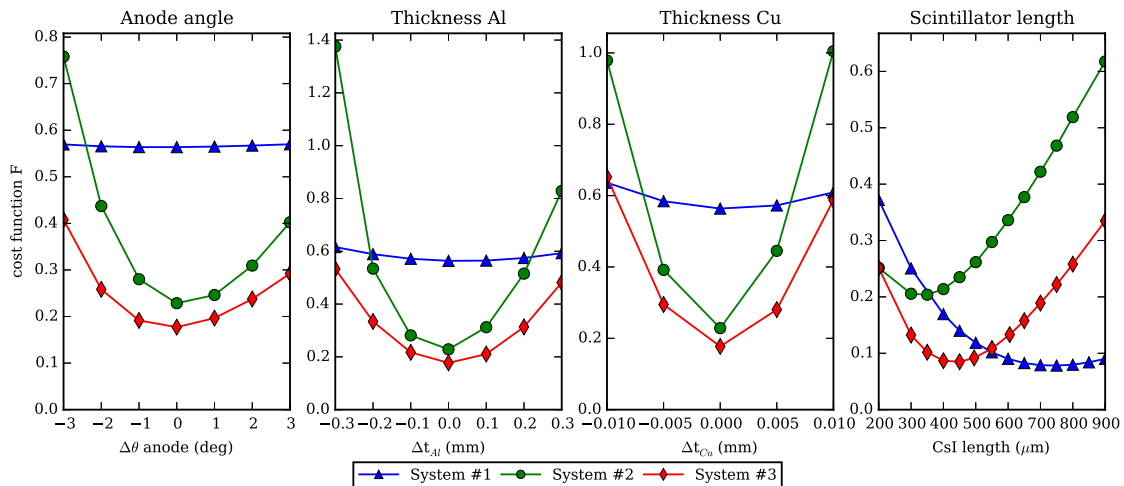

FIG. 4. Sensitivity analysis results in terms of the cost function as a function of the parameters of the source and the detector model. Variations were centered at the optimal values, summarized in Table II, determined previously in the model calibration stage.

using 2D dose detectors or applying the method developed by Randazzo and Tambasco[5] which is complementary to the current protocol. To compute the theoretical dose values in the 2D plane and thus, to account for the heel effect in the anode–cathode direction, analytic models of the heel effect that require few dose points measurements in the 2D plane might be used.[16]

According to the sensitivity analysis, very hardened beams (e.g., system #1) are less sensitive to variations in the source model parameters because anode angle or inherent filtration variations do not introduce significant changes in the photon yield. The detector response was sensitive to the scintillator length but it was characterized by a flat cost function around the optimum. In other words, the scintillator lengths in the 10% interval of the optimal CsI length would produce similar results.

The limitation of the current validation procedure is that when parametric models with many unknowns are used, like in the application example (Sec. 2.B), the experimental data are also used for the model calibration. In such cases, one needs to have independent sets of measurements for the validation. Otherwise, this procedure is only an indicator of the goodness of fit of our calibration. However, if the model of the CBCT scanner is precalibrated, this procedure can be exclusively used for validation. Presumably, the user would anyway further validate the model depending on its use, e.g., using a beam stop array for scatter simulations. To complement our sensitivity analysis, it would be of additional value to evaluate the impact of measurement uncertainties.

5. CONCLUSION

In this work, a calibration and validation procedure for any model of the source and the detector of a CBCT unit has been described. The experimental procedure requires instruments and equipments that are readily available in many clinical or research facilities. The protocol has been successfully applied to simple models of three commercial x-ray imaging systems.

ACKNOWLEDGMENT

CONFLICT OF INTEREST DISCLOSURE

The coauthors from RADART in Salzburg (Austria) are also part of the research and development department at med-Photon GmbH. The other coauthors have no relevant conflicts of interest to disclose.

a)Electronic mail: simon.rit@creatis.insa-lyon.fr

[1]G. Poludniowski, P. M. Evans, V. N. Hansen, and S. Webb, "An efficient Monte Carlo-based algorithm for scatter correction in keV cone-beam CT," Phys. Med. Biol. **54**(12), 3847–3864 (2009).

[2]G. X. Ding, P. Munro, J. Pawlowski, A. Malcolm, and C. W. Coffey, "Reducing radiation exposure to patients from kV-CBCT imaging," Radiother. Oncol. **97**(3), 585–592 (2010).

[3]P. Alaei and E. Spezi, "Imaging dose from cone beam computed tomography in radiation therapy," Phys. Med. **31**(7), 647–658 (2015).

[4]E. Spezi, P. Downes, E. Radu, R. Jarvis, and P. Downes, "Monte Carlo simulation of an x-ray volume imaging cone beam CT unit," Med. Phys. **36**(1), 127–136 (2009).

[5]M. Randazzo and M. Tambasco, "A rapid noninvasive characterization of CT x-ray sources," Med. Phys. **42**(7), 3960–3968 (2015).

[6]P. Downes, R. Jarvis, E. Radu, I. Kawrakow, and E. Spezi, "Monte Carlo simulation and patient dosimetry for a kilovoltage cone-beam CT unit," Med. Phys. **36**(9), 4156–4167 (2009).

[7]G. X. Ding, D. M. Duggan, and C. W. Coffey, "Characteristics of kilovoltage x-ray beams used for cone-beam computed tomography in radiation therapy," Phys. Med. Biol. **52**, 1595–1615 (2007).

[8]P. V. Granton, M. Podesta, G. Landry, S. Nijsten, G. Bootsma, and F. Verhaegen, "A combined dose calculation and verification method for a small animal precision irradiator based on onboard imaging," Med. Phys. **39**(7), 4155–4166 (2012).

[9]J. H. Hubbel and S. M. Seltzer, "Tables of x-ray mass attenuation coefficients and mass energy-absorption coefficients, 1 keV to 20 MeV for elements Z=1 to 92 and 48 additional substances of dosimetric interest," NISTIR 5632, National Institute of Standards and Technology (1995).

[10]J. Starman, J. Star-Lack, G. Virshup, E. Shapiro, and R. Fahrig, "A nonlinear lag correction algorithm for a-Si flat-panel x-ray detectors," Med. Phys. **39**(10), 6035–6047 (2012).

[11]G. Poludniowski, P. M. Evans, A. Kavanagh, and S. Webb, "Removal and effects of scatter-glare in cone-beam CT with an amorphous-silicon flat-panel detector," Phys. Med. Biol. **56**(6), 1837–1851 (2011).

[12]G. Poludniowski, G. Landry, F. DeBlois, P. M. Evans, and F. Verhaegen, "SpekCalc: A program to calculate photon spectra from tungsten anode x-ray tubes," Phys. Med. Biol. **54**(19), N433–N438 (2009).

[13]S. Jan, G. Santin, D. Strul, S. Staelens, K. Assié, and D. Autret, "GATE: A simulation toolkit for PET and SPECT," Phys. Med. Biol. **49**, 4543–4561 (2004).

[14]D. A. Roberts, V. N. Hansen, A. C. Niven, M. G. Thompson, J. Seco, and P. M. Evans, "A low Z linac and flat panel imager: Comparison with the conventional imaging approach," Phys. Med. Biol. **53**(22), 6305–6319 (2008).

[15]See supplementary material at http://dx.doi.org/10.1118/1.4961400 for the figures relative to the other systems.

[16]H. Braun, Y. Kyriakou, M. Kachelrieß, and W. A. Kalender, "The influence of the heel effect in cone-beam computed tomography: Artifacts in standard and novel geometries and their correction," Phys. Med. Biol. **55**, 6005–6021 (2010).